Computational Mechanics 24 (2000) 448–455 © Springer-Verlag 2000

Interfacial stress analysis for multi-coating systems using an advanced boundary element method

J. F. Luo, Y. J. Liu, E. J. Berger

Abstract This paper focuses on the interfacial stress analysis for multi-coating systems using an advanced boundary element method (BEM) developed earlier in [Luo JF, Liu YJ, Berger EJ (1998) Analysis of two-dimensional thin structures (from micro- to nano-scales) using the boundary element method. Comput. Mech. 22(5):404–412]. The advanced BEM with thin-body capabilities for two-dimensional linear elasticity is extended to general multi-domain problems and validated by the analytical solution of a special multi-coating problem. Detailed interfacial stress analysis for a two-layer coating system under uniform load distribution is investigated, through which the influence of coating thickness and material of the multi-coating system can be studied. The developed multi-coating analysis capability using the BEM provides not only a robust numerical tool for interfacial stress analysis of multi-coating systems with arbitrary coating thickness and number of coatings, but also the basis for future work concerning interface cracks, thermal effects and contact mechanics.

1 Introduction

The multi-coating system, which is the third generation coating system containing multiple layers of thickness in the micrometer and nanometer range, has obtained more and more applications in recent years (Subramanian and Strafford 1993), because of the satisfactory tribological performance under some extreme operating environment. However, the development made in the experimental research in thin coatings (Bhushan and Gupta 1991) (everything from thin coating and substrate interfacial strength and adhesion, to deposition rate and resultant hardness) underlies a general lack of modeling efforts which can accurately and efficiently predict the coating and thin film performance, including interfacial stresses and fatigue life. Although several analytical and numerical models (Chen 1971; Gupta and Wallowit 1974; Chiu and Hartnett 1983; King and O'Sullivan 1987; Komvopoulus 1989; Djabella and Arnell 1992; Kuo and Leer 1992; Mao et al. 1996; Bouzakis and Vidakis 1997; Bouzakis et al. 1997) for coating systems were developed by investigators in the last two decades, two limitations exist in these models. First, most of the existing models are restricted to a single thin layer system. Second, the modeling processes have been restricted to fairly well-defined geometry and loading conditions such as coating on an infinite half-space. Therefore the application of the models to practical components with complex geometry, such as bearings and gears, has been restricted. The finite element method (FEM) offers substantial potential in solving these problems for its flexible consideration of the geometry, loading type and number of coating layers. However, the aspect ratio issues associated with the FEM when applied to thin structures, as shown in (Luo et al. 1998), limit its application, since in a coating system the ratio of coating thickness and loading area may be in micro-scale (10^{-6}).

It has been shown in (Liu 1998; Luo et al. 1998) that the BEM can deal with ultra-thin structures very efficiently and accurately based on the elasticity theory, as long as the nearly-singular integrals existing in the BEM formulations are handled correctly. For the analysis of single-layer coatings or thin films using the developed 2-D BEM, much fewer boundary elements can be used to achieve the same accuracy as the FEM, including cases of non-uniform thickness (Luo et al. 1998). Accurate and stable numerical results of both displacements and stresses have been obtained in (Luo et al. 1998) for 2-D models of single-layer coatings or thin films, using the advanced BEM and with the total number of elements less than one hundred for a case which requires several thousand finite elements.

In this paper, the advanced boundary element method developed in (Luo et al. 1998) is extended to the multi-domain problems and applied to the interfacial stress analysis of multi-coating systems. The computer program in C++ is developed for general multi-domain problems and validated using the analytical solution of a special multi-coating problem. Detailed interfacial stress analysis for a two-layer coating system under uniform load distribution is investigated, through which the influence of coating thickness and material of the whole system can be studied. The developed BEM approach can provide not

Received 13 July 1999

J. F. Luo
Department of Mechanical Engineering,
University of California at Berkeley, Berkeley, CA 94720-1740

Y. J. Liu (✉), E. J. Berger
Department of Mechanical, Industrial and Nuclear Engineering,
University of Cincinnati, Cincinnati, OH 45221-0072

The first author (JFL) would like to acknowledge the financial support from the University of Cincinnati and the University of California at Berkeley. The second author (YJL) acknowledges the partial support of this research by the National Science Foundation under the grant CMS 9734949. The authors thank Ms. Nan Xu for her help on some of the example problems.

only a robust numerical tool for the interfacial stress analysis of multi-coating systems, but also the basis for further investigations of interfacial cracks, thermal effects and contact mechanics for the multi-coating system or various thin films.

2
The BEM formulation for multi-domain/multi-coating problems

In the following, the BEM formulation for general 2-D multi-domain problems is developed. Using the advanced boundary element method developed in (Luo et al. 1998), the formulation developed in this paper can be used to solve many multi-domain problems with large aspect (length to thickness) ratios. In addition, the number of domains or coatings can be arbitrary (limited only by computer memory and disk space).

The boundary integral equation (BIE) for 2-D elasticity problems, as shown below, can be applied in each domain (index notation is used for this BIE only, where repeated subscripts imply summation):

$$C_{ij}(P_0)u_j^{(\beta)}(P_0) = \int_\Gamma [U_{ij}^{(\beta)}(P,P_0)t_j^{(\beta)}(P) - T_{ij}^{(\beta)}(P,P_0)u_j^{(\beta)}(P)]\mathrm{d}\Gamma(P) \quad , \quad (1)$$

in which $u_j^{(\beta)}$ and $t_j^{(\beta)}$ are the displacement and traction fields, respectively; $U_{ij}^{(\beta)}(P,P_0)$ and $T_{ij}^{(\beta)}(P,P_0)$ the displacement and traction kernels (Kelvin's solution), respectively; P the field point and P_0 the source point; and Γ the boundary of the single domain. $C_{ij}(P_0)$ is a constant coefficient matrix depending on the smoothness of the curve Γ at the source point P_0 (see, e.g., Refs. (Mukherjee 1982; Cruse 1988; Banerjee 1994)). The superscript β on the variables in Eq. (1) signifies the dependence of these variables on the individual domain β.

There have been two major concerns in applying the BIE given in Eq. (1) to thin structures. The first concern is whether or not the conventional BIE (1) for elasticity problems can be applied to thin structures. It is well known in the BIE/BEM literature that BIE (1) will degenerate when it is applied to cracks or thin voids in structures because of the closeness of the two crack surfaces, see, e.g., Refs. (Cruse 1988; Krishnasamy et al. 1994). However, it has been shown that BIE (1) will not degenerate when it is applied to thin shell-like structures (Liu 1998), contrary to the case of crack-like problems. Thus the degeneracy issue should no longer be a concern when BIE (1) is applied to thin structures, once the second concern, i.e., the numerical difficulty, is addressed.

The numerical difficulty in BIE (1) is the nearly-singular integrals which arise in both crack-like and thin-structure problems. The integrals in Eq. (1) contain singular kernels of the orders $O(1/r)$ and $O(\ln r)$ in 2-D elasticity case, where r is the distance between the source point and the integration point on the boundary element. When the source point is very close to, but not on the element, although the kernels are regular in the mathematical sense, the values of the kernels change rapidly in the neighborhood of the source point. The standard Gauss-quadrature is no longer practical in this case since a large number of integration points are needed in order to achieve the required accuracy. Analytical and numerical methods have been devised in Refs. (Liu et al. 1993; Liu 1998; Luo et al. 1998) to compute these nearly-singular integrals accurately and efficiently, for both 2-D and 3-D thin structures with the thickness to length ratio as small as in micro- or nano-scales.

To apply the conventional BIE (1) and the method dealing with the nearly singular integrals discussed in (Luo et al. 1998), three main assumptions are made: (1) The multi-coating system is composed of one or more homogeneous elastic thin layers bonded to each other, and, in turn, to the substrate. Each layer and the substrate are taken as having their own distinct mechanical properties; (2) The state of deformation for the coating system is plane strain, so that the system could be considered in two dimensions. This assumption holds well for line contacts, such as those which arise in gears and roller bearings; (3) Strains are assumed small and elastic, leading to the usual linear elastic theory.

The advanced boundary element method in (Luo et al. 1998) is based on one homogeneous, isotropic and linear elastic medium. In multi-coating systems, several layers with each one being homogeneous, isotropic and linear elastic, must be analyzed. In such situations, the final set of equations for the whole region should be obtained by assembling the set of equations for each coating using the traction equilibrium and displacement compatibility conditions on the interfaces.

Figure 1 shows two elastic bodies, one rectangular and one circular substrates, coated with n elastic layers (the developed approach is applicable to coating systems with arbitrary geometries). The boundary and/or interface conditions for each layer can be written as follows:
1. On the boundary (external surface) of a coating layer, the traction must be given, such as:

$$T_\mathrm{n} = p_\mathrm{n}, \; T_\mathrm{t} = p_\mathrm{t} \qquad (2)$$

where T_n and T_t are the normal and tangential components of the traction, p_n and p_t the applied loads in the normal and tangential direction, respectively. In addition, the coating system should be constrained (with specified displacement) at some other locations on the boundary.

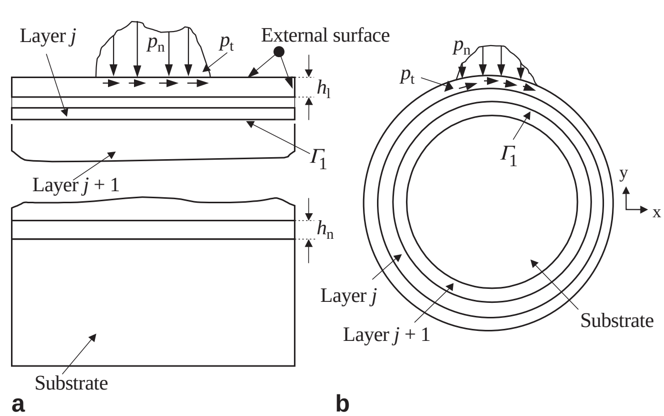

Fig. 1a,b. Coordinates and notation for two multi-coated elastic solids

2. On every interface Γ_I between layers j and $j+1$, the normal and tangential tractions and displacements from both sides of the interface satisfy:

$$T_{\mathrm{In}} = T^j_{\mathrm{In}} = -T^{j+1}_{\mathrm{In}}, \quad T_{\mathrm{It}} = T^j_{\mathrm{It}} = -T^{j+1}_{\mathrm{It}} \quad , \tag{3}$$

$$U_{\mathrm{In}} = U^j_{\mathrm{In}} = U^{j+1}_{\mathrm{In}}, \quad U_{\mathrm{It}} = U^j_{\mathrm{It}} = U^{j+1}_{\mathrm{It}} \quad , \tag{4}$$

where the subscript In indicates interface (I) and normal (n) component, and subscript It indicates interface (I) and tangential (t) direction.

It is important to note that only the perfectly bonded parts of the interface satisfy the above traction equilibrium and displacement compatibility conditions. The non-perfectly bonded parts, say, an interface crack, will be considered as an additional boundary of each layer (similar to the external boundary of each layer) and the tractions and displacements associated with them will not be coupled together in the final equations.

First, the two layers j and $j+1$ with interface Γ_I, as shown in Fig. 1, are analyzed. For the jth layer one has the following discretized form of the BIE given in (1):

$$[H^j \quad H^j_I]\begin{Bmatrix} U^j \\ U^j_I \end{Bmatrix} = \begin{bmatrix} G^j & G^j_I \end{bmatrix}\begin{Bmatrix} T^j \\ T^j_I \end{Bmatrix} \quad , \tag{5}$$

where U^j_I and T^j_I are the interface displacements and tractions of layer j on the interface Γ_I, U^j and T^j the displacements and tractions of the layer j on the remaining surfaces. Note that for the jth thin layer the coefficient matrices H^j, H^j_I, G^j and G^j_I in above equations are evaluated using the advanced boundary element method developed in (Luo et al. 1998), which can handle the nearly-singular integrals accurately for 2-D thin structures. Specifically, in Ref. (Luo et al. 1998), the nearly-singular integrals (line integrals for 2-D problems) were transformed into function evaluations at the two end points of the element of integration. In addition, a new nonlinear coordinate transformation was developed to further increase the numerical accuracy for nearly weakly-singular integrals. By employing these new techniques, the nearly singular integrals in 2-D BEM can be evaluated very accurately, even if the distance of the source point to the element of integration, normalized by the element length, is in the orders of 10^{-6}–10^{-9} (Luo et al. 1998).

Similarly, for the layer $j+1$, we have

$$[H^{j+1} \quad H^{j+1}_I]\begin{Bmatrix} U^{j+1} \\ U^{j+1}_I \end{Bmatrix} = \begin{bmatrix} G^{j+1} & G^{j+1}_I \end{bmatrix}\begin{Bmatrix} T^{j+1} \\ T^{j+1}_I \end{Bmatrix} \quad , \tag{6}$$

where U^{j+1} and T^{j+1} are the displacements and tractions of the layer $j+1$ on the external surface, U^{j+1}_I and T^{j+1}_I the interface displacements and tractions of the layer $j+1$ on the perfectly bonded parts of interface Γ_I.

According to the equilibrium and compatibility conditions (3) and (4) at an interface, one has the following relations at the interface Γ_I:

$$U_I \equiv U^j_I = U^{j+1}_I, \quad T_I \equiv T^j_I = -T^{j+1}_I \quad .$$

Hence, Eqs. (5) and (6) can be rewritten as:

$$[H^j \quad H^j_I \quad -G^j_I]\begin{Bmatrix} U^j \\ U_I \\ T_I \end{Bmatrix} = G^j T^j \quad ,$$

and

$$[H^{j+1} \quad H^{j+1}_I \quad G^{j+1}_I]\begin{Bmatrix} U^{j+1} \\ U_I \\ T_I \end{Bmatrix} = G^{j+1} T^{j+1}$$

respectively.

Coupling of the above two equations yields:

$$\begin{bmatrix} H^j & H^j_I & -G^j_I & 0 \\ 0 & H^{j+1}_I & G^{j+1}_I & H^{j+1} \end{bmatrix}\begin{Bmatrix} U^j \\ U_I \\ T_I \\ U^{j+1} \end{Bmatrix} = \begin{bmatrix} G^j & 0 \\ 0 & G^{j+1} \end{bmatrix}\begin{bmatrix} T^j \\ T^{j+1} \end{bmatrix} \quad . \tag{7}$$

More equations will be added to this system in a similar way for other layers and the substrate. The system still needs to be reordered according to the prescribed displacement and traction boundary conditions. An advantage for the BEM as applied to multi-domain problems is that both traction equilibrium and displacement compatibility conditions between layers are explicitly satisfied, as compared to the FEM, in which only the displacement compatibility condition is explicitly satisfied. Moreover, note that the above equations are now banded. For an n-layer coating system, the final global system matrix, after applying the boundary conditions and subsequently reordering, will look like the one shown in Fig. 2.

A BEM software based on the above formulation has been developed using the object-oriented programming (OOP) technique, which was extended readily from the C++ program developed for single domain problems in (Luo et al. 1998). There are no limitations on layer and node numbers of the multi-domain/multi-coating models to apply the above BEM software, except the storage capacity. The developed code has been shown to be very efficient on both UNIX workstations and MS Windows-based PCs. It is also very accurate, as is demonstrated next by several numerical examples.

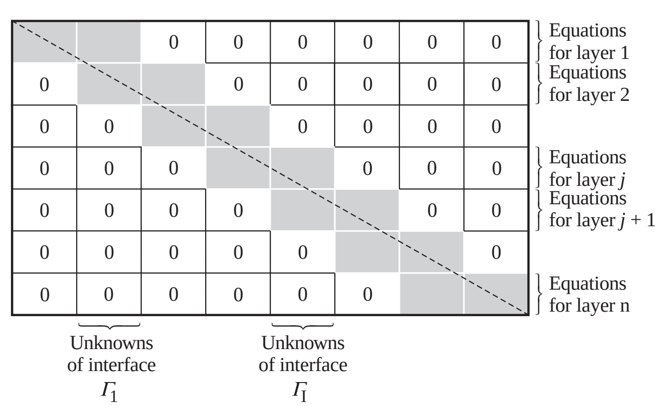

Fig. 2. The final system matrix for an n-layer coating system

3 Numerical examples

3.1 Validation of the BEM model

To verify the BEM formulation and the computer code developed for the multi-domain problems, a circular shaft with two layers of coatings is studied first, for which the analytical solution is derived (cf., the analytical solution in (Liu et al. 1998) for a different boundary condition).

Figure 3 shows two layers of coatings with different materials and thickness on a rigid shaft (Young's modulus of outside coating/Young's modulus of inner coating = 1/2 and Poisson ratio of outside coating/Poisson ratio of inner coating = 1). It is assumed here that the layers of coatings and shaft are perfectly bonded to each other. The problem is an extension from the uniform-thickness coating studied in (Luo et al. 1998), where only one layer of coating is studied. The shaft and the two coatings have outer radii r_s, r_{c1} and r_{c2}, respectively; see Fig. 3. It is assumed that the coatings are free to expand laterally except at the interface to the rigid shaft, but are constrained axially so that a condition of plane strain relative to x–y plane exists. The thickness of inner coating $h_{c1} = r_{c1} - r_s = 1.1$ mm $-$ 1.0 mm = 0.1 mm, which is constant in this study, while the thickness of outside coating h_{c2} changes from 0.1 mm to 1.0×10^{-4} mm (0.1 μm). In the BEM model, a total of 24 quadratic boundary elements are used to model the two coatings. Note that only 48 nodes are needed in modeling the whole system since the nodes over the interfaces are shared by both coatings. Also note that no re-meshing is needed when the thickness h_{c2} decreases from 0.1 mm to 0.1 μm. It is assumed that the coating system is loaded by a uniform pressure p which is distributed around the circumference of the outside coating. The boundary conditions for the displacement, considering the rigid shaft assumption, are $u_r = u_\theta = 0$ for all nodes at the shaft-coating interface.

Figure 4 shows the magnitude of radial stress σ_{rr} predictions at points A and B, respectively, by the developed BEM and the analytical solution (Liu et al. 1998). It can be seen that when the thickness of the outside coating changes from 0.1 mm to 10^{-4} mm (0.1 μm), the errors of the BEM predictions are still smaller than 1%. The results clearly demonstrate the validity of the developed BEM for multi-coating problems.

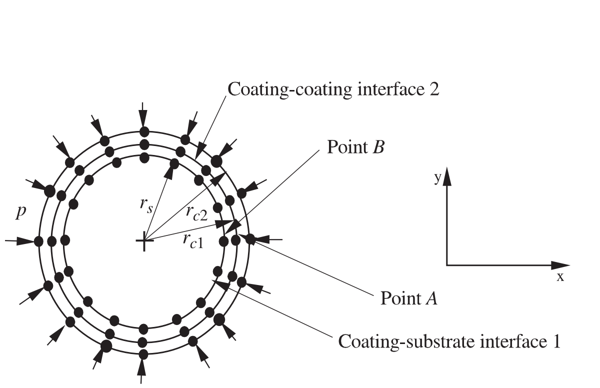

Fig. 3. Cross-section of a shaft with two layers of coatings

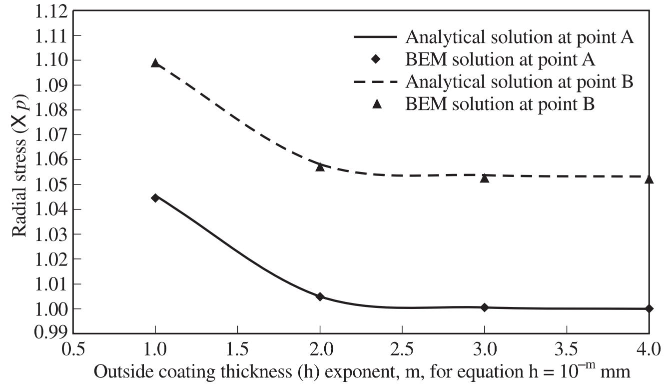

Fig. 4. Radial stress (σ_{rr}) at points A and B

3.2 Interfacial stress analysis for a two-layer coating system under uniform load

The developed BEM is used to perform interfacial stress analysis for the following multi-coating structures and to study the change of interfacial stresses as a function of material properties and coating thicknesses.

Figure 5 shows a symmetric two-layer coating system under a uniformly distributed load p of half-width A, where H_{c1} is the thickness of the outside coating, H_{c2} the thickness of the inside coating, H_s the substrate height, L the structure length, E_{c1} Young's modulus of outside coating, E_{c2} Young's modulus of inside coating, and E_s Young's modulus of the substrate. It is assumed that the structure length, the contact half width and the Poisson's ratio of coatings and substrate are fixed ($h = H_s + H_{c1} + H_{c2} = 20$ mm, $L = 20$ mm, $A = 1$ mm, $\upsilon = 0.3$), while the coating thickness changes from 1 mm to 10 μm and the Young's modulus ratio (E_{c1}/E_s, E_{c2}/E_s) varies between 1 and 100. Because the dimensions of the whole system ($h = 20$ mm, $L = 20$ mm) are large compared with the dimensions of the loading area ($A = 1$ mm), analytical solution of the interfacial stresses may be calculated to good approximation by considering the whole system as an elastic half-space, when the materials of the coatings and substrate are the same (Johnson 1985). The points c and d, see Fig. 5, are points corresponding to the edge of the distributed load at the coating-coating interface and coating-substrate interface, respectively. When the coatings are very thin (as $H_{c1},\ H_{c2} \to 0$), the normal stresses at these two points approach $p/2$ (Boresi and Chong 1987;

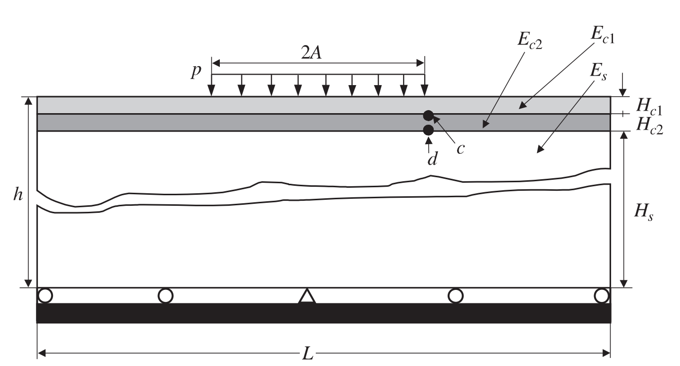

Fig. 5. A multi-coating system under uniform load of half-width A

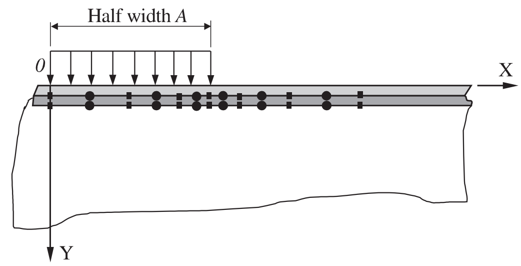

Fig. 6. Interfacial mesh close to the contact area

Johnson 1985), while the shear stresses approach p/π (Johnson 1985) if the coating and substrate materials are the same. This can be used to check the validity of the BEM solutions when analytical solutions are not available for different coating/coating/substrate material combinations.

In the following examples, the outside surfaces and interfaces of the BEM model are discretized with 115 and 134 quadratic elements, respectively. In order to capture the rapid stress variations around the edges of the load (contact) area and to obtain accurate solution, finer meshes are used near the edges, see Fig. 6. In addition, no re-meshing is done when the thicknesses of coatings change from 0.1 mm to 0.01 mm (10 μm).

(a) Interfacial stress with same/different coating materials

It is assumed that the thickness of both coatings is kept as 0.1 mm ($H_{c1}/A = 1/10$, $H_{c2}/A = 1/10$) and the coatings and substrate are perfectly bonded to each other. First, consider the case that both coatings are composed of the same materials as the substrate, for which an analytical stress solution exists (see (Johnson 1985), p. 21). For the uniform loading case, while the stress gradients at the edges of contact are large, the stresses do not become singular (as in some rigid indenter problems). All the stress components are finite in this case. However, the shear stress has a jump from zero at the surface to p/π just below the loading edge (see (Johnson 1985), p. 25). Actually, in this special case, the "interfacial" stresses are in fact the internal stress components in the single material. The multi-domain BEM is applied here simply to obtain these stresses inside this single material domain, in order to compare with the analytical solution.

Figure 7 shows the BEM normal stress (σ_{yy}) predictions compared with the analytical solution in the neighborhood of the contact area. Note that the normal "interfacial" stress on points c and d are close to $p/2$. Figure 8 shows the BEM shear stress (τ_{xy}) predictions compared with the analytical solution. It is noticed that the peak values of the shear stresses (at the edge of loading) are very close to p/π which is the analytical value for the point just beneath the loading edge (Johnson 1985). These results demonstrate that the BEM solution is extremely accurate, which verifies again the accuracy of the developed algorithm in (Luo et al. 1998) and the multi-domain BEM formulation developed in this paper.

In Fig. 9, the Young's modulus ratio of the outside coating and the substrate is fixed at 2 while the Young's modulus ratio of the inside coating and the substrate

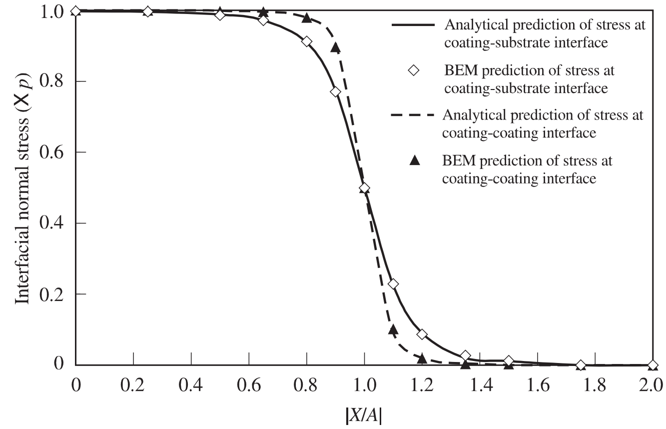

Fig. 7. Interfacial normal stress (σ_{yy}) prediction when $E_{c1} = E_{c2} = E_s$

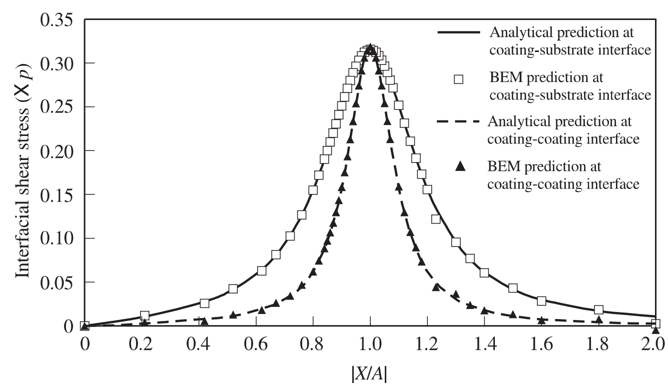

Fig. 8. Interfacial shear stress (τ_{xy}) prediction when $E_{c1} = E_{c2} = E_s$

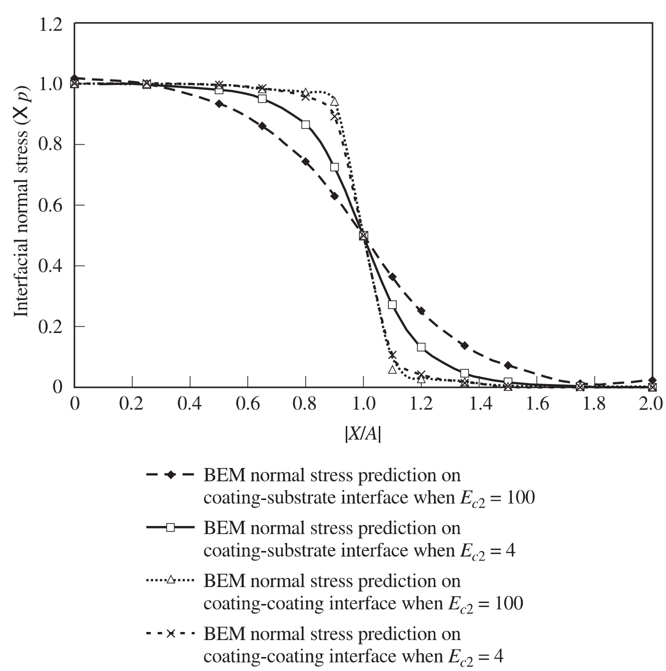

Fig. 9. Interfacial normal stress (σ_{yy}) prediction with different coating materials

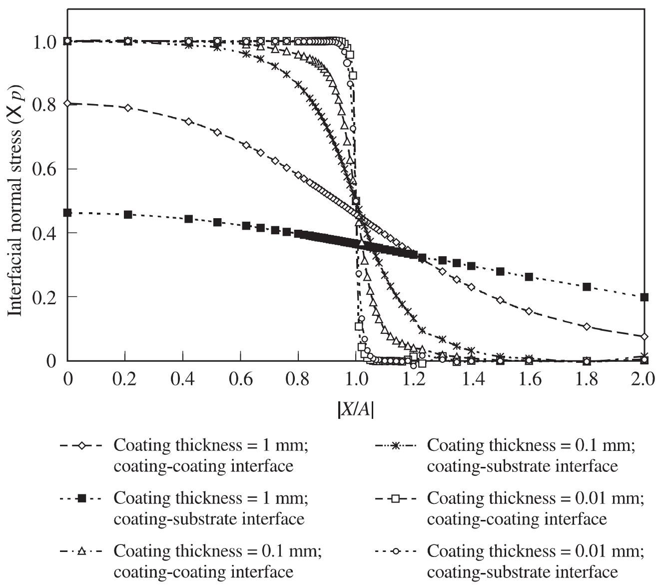

Fig. 10. Interfacial normal stress (σ_{yy}) prediction with different coating thicknesses

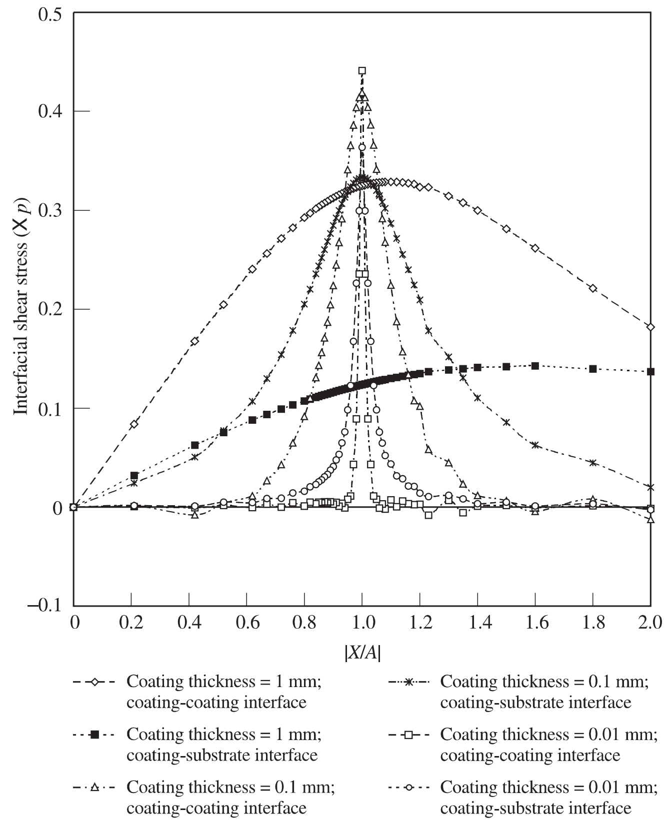

Fig. 11. Interfacial shear stress (τ_{xy}) prediction with different coating thicknesses

changes from 4 to 100. The thickness of both coatings is still kept as 0.1 mm. It is found that changing materials of the inside coating has a larger influence on coating-substrate interfacial stress distribution than on coating-coating interfacial stress distribution.

(b) Interfacial stress with different coating thicknesses
In this example, the Young's modulus ratios of coatings and substrate are kept as $E_s/E_{c1}/E_{c2} = 1/4/2$. The thicknesses of both coatings change from 1 mm to 10 μm. Figures 10 and 11 show the interfacial stress distributions for different coating thickness. When coatings become thinner, the interfacial stress distribution is closer and closer to the loading distribution even if the materials of coatings and substrate are different from each other, except that the shear stresses near the edge of the loading exhibit a rapid transition as observed in Fig. 11. This rapid rise in the shear stresses near the loading edge is similar to that in the same material case (Fig. 8), only with a sharper rise and larger (but still finite) peak value when the coating thicknesses become thinner. There are no analytical solutions available in the literature, to the best of the authors' knowledge, for this multi-coating case. It is pointed out that for smaller thicknesses of the coatings, no re-meshing or only a slightly finer mesh in the neighborhood of loading edges is needed in order to account for the sharp stress changes in that region.

4
Discussion

Based on the advanced BEM developed in (Luo et al. 1998) for 2-D linear elasticity, the BEM formulation and computer code for multi-coating systems are developed in this paper. Compared with earlier analytical methods and the FEM (Chen 1971; Gupta and Wallowit 1974; Chiu and Hartnett 1983; King and O'Sullivan 1987; Komvopoulus 1989; Djabella and Arnell 1992; Kuo and Leer 1992; Mao et al. 1996; Bouzakis and Vidakis 1997; Bouzakis et al. 1997), the developed BEM has the following advantages: (1) Based on discretizations of only the boundaries and interfaces, the BEM can model any kind of coating systems without limitations on the geometry. (2) Compared with the FEM, the BEM meshes use fewer elements and therefore less computation time and memory are required. More importantly, no or less re-meshing is needed when the coating thickness is changed, and so a systematic optimization of coating thickness is much easier and faster than that by the FEM. Moreover, with nearly-singular integrals evaluated efficiently, the BEM can deal with thin coatings, even if they have micro-scale thickness, using only a few elements. The possibility to do the analysis for the whole range of thickness makes the optimization of a coating system much easier to conduct using the BEM. (3) Furthermore, for single- or multi-layer problems, the overall number of finite elements will always be driven by the layer thickness (the element aspect ratio restriction), regardless of the stress conditions. For a multi-layer problem, the FEM can be very costly. However, the BEM discretization will always be driven by the stress gradients, with a much lower sensitivity to layer thickness, since the nearly-singular integrals arising due to the thin geometry can be evaluated accurately without the need to reduce the element sizes. As a result, the BEM will perform more efficiently than the FEM which requires the reduction of element sizes due to the element aspect ratio restriction, particularly for the analysis of so-called "third-generation" coatings. Even for the case of extremely large stress gradients, as with stress singularities at the contact edges associated with (rigid) indenter problems, the BEM will require mesh refinement only in the vicinity of the contact edges, with relaxed meshing requirements elsewhere. (4) The developed BEM approach has the potential to be the best choice for interfacial crack analysis for thin coating systems. It is difficult for the earlier methods mentioned above to deal with interfacial cracks effectively even if the geometry and loading type studied are simple enough. The advanced BEM developed in this paper, however, seems to be a very promising method for interfacial crack analysis, as will be elaborated further below.

When analyzing the interfacial stresses of multi-coating system, it is often necessary to consider the effect of interface cracks (or debonding at the interfaces). When the coatings are ultra-thin and perfectly bonded to each other, the interfacial stresses reproduce the external loading distribution. However, if cracks exist at the interface, the stress distribution will change dramatically, especially near the cracks. It is difficult to find analytical solutions, except for simple geometry (Suo and Hutchinson 1990), to deal with the interface cracks in real coating systems with arbitrary loading and geometries, and therefore experimental and numerical methods have to be used. Although the FEM can be applied, theoretically, to interface crack analysis of structures with arbitrary geometry, difficulties still exist in modeling interface cracks by the FEM for multi-coating systems. The major difficulty is that a large number of elements must be used in the domain close to the crack to capture the rapid stress changes. It is long believed that the BEM is more efficient and accurate in crack modeling due to the boundary-only discretizations and its semi-analytical nature (Cruse 1988). However, the previous BEM models cannot be applied readily to thin structures such as multi-coating systems, because of the nearly-singular integral problem (Liu 1998; Luo et al. 1998). The BEM approach developed in this paper provides a well-suited method to model interface cracks in multi-coating systems. Even though the small scale yielding at the crack tip needs to be considered for thin films and coatings, due to the small thickness of the films or coatings, it is still advantageous to use the BEM. Domain discretizations (using 2-D elements) are only necessary for the plastic zone which is in general a small portion of the whole domain, and boundary discretizations (using 1-D elements) are still dominant in the entire domain (Mukherjee 1982). Detailed study on the interface cracks using the developed BEM is underway and will be reported in another paper.

The BEM tools developed for multi-coating systems in this research also offer great promise in analysis and design of many contact components, including gears, cams, and bearings. In Hertz-type contact systems, the location of maximum principal shear stress is sub-surface; the actual depth in multi-coating systems depends upon loading conditions (including surface shear traction) and coating material and thickness. The BEM tools presented here offer new options in coating design by allowing fast and accurate calculation of interface stresses. Multi-coated components can be designed such that the maximum shear stress location is not coincident with a coating-coating or coating-substrate interface. With further developments of the BEM procedures, including the addition of contact mechanics solutions, the tools developed here will provide great flexibility in contact stress analysis.

From the numerical examples and the above discussions, it is concluded that the developed BEM is an accurate and efficient numerical method for modeling multi-coating systems. In the follow-up work, more realistic coating models including thermal effects and contact mechanics can be considered. The work in this paper provides a solid basis for these research topics.

References

Banerjee PK (1994) The Boundary Element Methods in Engineering. New York, McGraw-Hill

Bhushan B, Gupta BK (1991) Handbook of Tribology: Materials, Coatings, and Surface Treatments. New York, McGraw-Hill

Boresi AP, Chong KP (1987) Elasticity in Engineering Mechanics. New York, Elsevier

Bouzakis K-D, Vidakis N (1997) Prediction of the fatigue behaviour of physically vapour deposited coatings in the ball-on-rod rolling contact fatigue testing, using an elastic-plastic finite element method simulation. Wear 206:197–203

Bouzakis K-D, Vidakis N, Leyendecker T, Erkens G, et al (1997) Determination of the fatigue properties of multilayer pvd coatings on various substrates, based on the impact test and its FEM simulation. Thin Solid Films 308–309:315–322

Chen WT (1971) Computation of stresses and displacements in a layered elastic medium. Int. J. Eng. Sci. 9:775–800

Chiu YR, Hartnett MJ (1983) A numerical solution for layered solid contact problems with applications to bearings. ASME J. Lubrication Technol. 105:585–590

Cruse TA (1988) Boundary Element Analysis in Computational Fracture Mechanics. Dordrecht, Boston, Kluwer Academic Publishers

Djabella H, Arnell RD (1992) Finite element analysis of the contact stresses in an elastic coating on an elastic substrate. Thin Solid Films 213:205–219

Gupta PK, Wallowit JA (1974) Contact stresses between an elastic cylinder and a layered elastic solid. ASME J. Lubrication Technol. 96:250–257

Johnson KL (1985) Contact Mechanics. Cambridge, Cambridge University Press

King RB, O'Sullivan TC (1987) Sliding contact stresses in a two-dimensional layered elastic half-space. Int. J. Solids & Structures 23:581–597

Krishnasamy G, Rizzo FJ, Liu YJ (1994) Boundary integral equations for thin bodies. Int. J. Num. Meth. Eng. 37:107–121

Komvopoulus K (1989) Elastic-plastic finite element analysis of indented layered media. ASME J. Tribology 111:430–439

Kuo CH, Leer LM (1992) Contact stress analysis of a layered transversely isotropic half-space. ASME J. Tribology 114:253–262

Liu YJ (1998) Analysis of shell-like structures by the boundary element method based on 3-D elasticity: formulation and verification. Int. J. Num. Meth. Eng. 41:541–558

Liu YJ, Xu N, Luo J (1998) Modeling of interphases in fiber-reinforced composites under transverse loading using the boundary element method. Trans. ASME J. Appl. Mech. to appear

Liu YJ, Zhang D, Rizzo FJ (1993) Nearly singular and hypersingular integrals in the boundary element method. In: Boundary Elements XV, Worcester, MA, Computational Mechanics Publications: 453–468

Luo JF, Liu YJ, Berger EJ (1998) Analysis of two-dimensional thin structures (from micro- to nano-scales) using the boundary element method. Comput. Mech. 22:404–412

Mao K, Sun Y, Bell T (1996) A numerical model for the dry sliding contact of layered elastic bodies with rough surfaces. STLE Tribology Trans. 39:416–424

Mukherjee S (1982) Boundary Element Methods in Creep and Fracture. New York, Applied Science Publishers

Subramanian C, Strafford KN (1993) Review of multicomponent and multilayer coatings for tribological applications. Wear 85–95

Suo Z, Hutchinson JW (1990) Interface crack between two elastic layers. Int. J. Fracture 43:1–18